Meteoritics & Planetary Science 39, Nr 10, 1699–1720 (2004)
Abstract available online at http://meteoritics.org

Distribution and stratigraphy of basaltic units in Maria Tranquillitatis and Fecunditatis: A Clementine perspective

D. RAJMON[1, 2*] and P. SPUDIS[2#]

[1]Department of Geosciences, University of Houston, Houston, Texas 77204, USA
[2]Lunar and Planetary Institute, Houston, Texas 77058, USA
[*]Present address: Shell International E&P, Houston, Texas 77025–1299, USA
[#]Present address: John Hopkins University, Applied Physics Laboratory, Laurel, Maryland 20723–6099, USA
[*]Corresponding author. E-mail: drajmon@yahoo.com

(Received 19 March 2003; revision accepted 5 August 2004)

Abstract–Maria Tranquillitatis and Fecunditatis have been mapped based on Clementine image mosaics and derived iron and titanium maps. Impact craters served as stratigraphic probes enabling better delineation of compositionally different basaltic units, determining the distribution of subsurface basalts, and providing estimates of total basalt thickness and the thickness of the surface units. Collected data indicate that volcanism in these maria started with the eruption of low-Ti basalts and evolved toward medium- and high-Ti basalts. Some of the high-Ti basalts in Mare Tranquillitatis began erupting early and were contemporaneous with the low- and medium-Ti basalts; these units form the oldest units exposed on the mare surface. Mare Tranquillitatis is mostly covered with high-Ti basalts. In Mare Fecunditatis, the volume of erupting basalts clearly decreased as the Ti content increased, and the high-Ti basalts occur as a few patches on the mare surface. The basalt in both maria is on the order of several hundred meters thick and locally may be as thick as 1600 m. The new basalt thickness estimates generally fall within the range set by earlier studies, although locally differ. The medium- to high-Ti basalts exposed at the surfaces of both maria are meters to tens of meters thick.

INTRODUCTION

Knowing the three-dimensional distribution of mare basalt infill is an important prerequisite for constraining the magmatic and thermal history of the Moon (Basaltic Volcanism Study Project 1981). Estimating the volume of the Ti-rich lava also determines ilmenite reserves—a potential lunar oxygen resource through ilmenite reduction by heated hydrogen (e.g., Gibson and Knudsen 1985; Chambers et al. 1995).

Mare basalts have been mapped using a variety of techniques, including photogeologic, X-ray, γ-ray, and spectral data. Photogeologic data provide morphologic information and counting craters on mare surfaces allows the determination of relative and absolute ages. The available broadband (black & white) images from Earth-based telescopes, Lunar Orbiters, or Apollo cannot distinguish different types of basalts. X-ray and γ-ray data from Apollo or Lunar Prospector provide information on composition, but only at low spatial resolutions. Spectral data provided a base for a detailed spectral classification, initially, at the low spatial resolution of telescopic observation (e.g., Pieters 1978; Johnson et al. 1991) and, more recently, at higher resolution of multispectral image data from Galileo and Clementine, and Earth-based telescopes (e.g., Greeley et al. 1993; Melendrez et al. 1994; Williams et al. 1995; Staid et al. 1996; Giguerre et al. 2000; Hiesinger et al. 2000; Kodama and Yamaguchi 2003). Correlation of spectral properties with the composition of lunar samples has allowed a qualitative interpretation of the defined spectral units in terms of chemical composition. Algorithms for calculation of iron and titanium content from the Clementine multispectral data (Lucey et al. 1995; Blewett et al. 1997; Lucey et al. 1998; Lucey et al. 2000a) allowed a significant extension of a database used for mapping. Using these techniques, we have mapped basaltic units in Maria Tranquillitatis and Fecunditatis based on chemical composition of basalts excavated by individual impact craters rather than based on bulk composition of soil. This mapping is at an order of magnitude higher spatial resolution than the mapping of Hiesinger et al. (2000) and Staid et al. (1996), and at about the same resolution as the work of Kodama and Yamaguchi (2003). The geochemical data allow new independent estimates of basalt thickness in the maria.

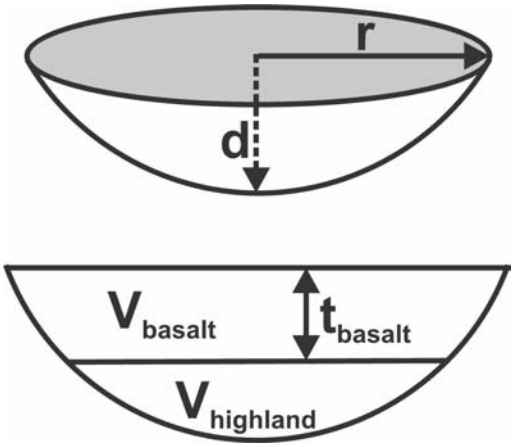

Fig. 1. Illustration of FeO mixing model used for calculation of total basalt thickness. r = radius, d = excavation depth, V = volume, t = thickness; all parameters are for transient cavity.

METHOD

We processed mosaics of Clementine images covering Maria Tranquillitatis and Fecunditatis at wavelengths of 415, 750, and 950 nm, respectively. All mosaics were processed at a resolution of 250 m/pixel, although, at some areas, the resolution of the original data appeared lower. Sinusoidal projections of the mosaics, as well as all derived maps, are centered on longitude +31º for M. Tranquillitatis and +50º for M. Fecunditatis. The mosaics were then combined to generate several image products. "True" color image has red, green, and blue channels controlled by 950, 750, and 415 nm mosaics, respectively. This composite approximates the true color of the Moon. False color image has channels controlled by ratios of the monochromatic mosaics (R = 750/415, G = 750/950, B = 415/750). False color image exaggerates color differences between different geological units. Mature highland material appears red, excavated highland blue, low-Ti basalts orange, high-Ti basalts blue, and excavated basalts yellow to green. FeO and TiO_2 concentration maps were calculated from the 415 and 750 nm mosaics using equations of Lucey et al. (2000a). In addition to Clementine data, we also used Lunar Orbiter IV images and lunar maps of the LM and LAC series for better topography and morphology of the studied area.

We mapped all of the compositional variations within the maria integrating information from all available image layers. This step yielded a large number of units. We then measured average FeO and TiO_2 concentration in soil by random sampling with 5 × 5 pixel box, estimated basalt composition for each unit from ejecta of young craters excavating only basalt, and classified each unit according to the gathered information.

Impact craters serve as probes of mare stratigraphy to estimate composition of top and buried basalt units and to estimate basalt thickness. High FeO contrast between mare basalt and highland substrate allows identification of craters that penetrated basalt. Ejecta of such craters have intermediate concentration of FeO because of mixing between basalt and highland substrate. Average FeO concentrations in continuous ejecta were estimated from the iron map. We applied a simple linear mixing model, with average highland and mare basalt as chemical end members, to calculate fractions of excavated basalt and highland substrate. The fractions were fit back into a spherical cavity to estimate the total pre-impact thickness of mare basalt for each crater (Fig. 1). Excavation depths were estimated from final crater diameters assuming an effective depth to diameter ratio (h/Dt) of the excavation cavity of 0.1–0.14 (Maxwell 1977; Grieve et al. 1981) and a transient diameter to final diameter ratio (Dt/D) of 0.84 for simple craters and 0.5–0.65 for complex craters (Melosh 1989). FeO concentration for the basalt (18.0–18.7 wt%) and highland (4 wt%) endmembers was selected based on evaluation of the iron map and available analytical data for Apollo 11 and Luna 16 samples (Essene et al. 1970; Heiken et al. 1991). The iron map is accurate to ±1.15 wt% FeO (1 σ) (Lucey et al. 2000a). The reading of ejecta composition from the map is complicated in many cases by uncertainty in the continuous ejecta extend, partial flooding of the ejecta with younger lava, small younger impact craters within the ejecta excavating only basalt, etc. The FeO reading is therefore associated with about 1 wt% FeO error. Increase in FeO reading from ejecta by 1 wt% FeO causes an increase in thickness by 15% (for strong highland contamination) to 65% (for almost pure basaltic ejecta). Increase of h/D_t ratio from 0.1 to 0.14 causes an increase in thickness by 40–50%, in some cases but also up to 60%. Increase in FeO by 1 wt% for the basalt endmember causes a decrease of thickness by 10–15%. Increase in FeO by 1 wt% for highland endmember decreases the thickness by 1–15% (Fig. 2).

Certain error may be introduced in the FeO map due to topographic shading effect (Lucey et al. 1998). The induced "topographic error" is a function of phase angle (roughly corresponding to latitude in Clementine data) and local slope (Lucey et al. 1998). The studied regions are located between –10º and +18º latitude in M. Tranquillitatis, and between –15º and +10° in M. Fecunditatis, which makes the "topographic error" significant only for steep slopes, such as crater walls. FeO readings from ejecta blankets are virtually free of this error.

A similar approach was applied to the titanium map, which allows distinguishing among basalts with different TiO_2 contents. Craters that penetrated only the top basalt layer provide composition of this layer. Larger craters that penetrated deeper into the buried basalt layer with different TiO_2 content provide information about this buried layer. This approach is complicated by small size of the craters probing just the top basalt. They are typically covered by just a few pixels, not allowing a clear distinction between crater floor

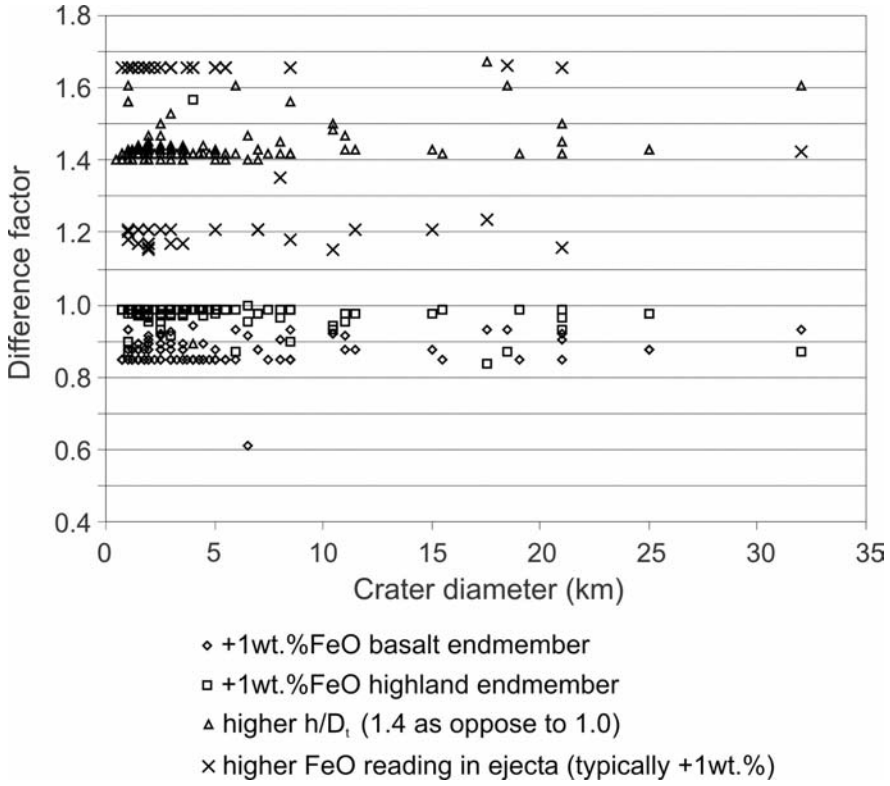

Fig. 2. Analysis of uncertainty in total basalt thickness estimates derived from craters in Mare Tranquillitatis. The difference factor indicates how much a thickness estimate changes in response to a change of parameters used in calculation.

and steep walls. In cases when the steep slopes cannot be avoided, the TiO_2 readings can be affected by the "topographic error," which may reach about 2.5 wt% for the studied regions (Lucey et al. 1998). The underlying assumption of our approach is that the basalt stratigraphy can be described with a model of two basalt layers. In reality, the mare fill probably consists of multiple layers with varying titanium contents. Except for a few cases discussed later, we were not able to resolve more than two basalt layers. An unknown amount of mixing between the top and the buried unit(s) is also affecting the readings because the thickness of the top layer is not known. Therefore, estimation of both the thickness of the top layer and the composition of the buried layer requires iteration through comparison of a number of craters of different sizes and assumption that the thickness does not vary much over short distance. Because of the "two-layer" assumption and the "mixing" uncertainty, the titanium content tends to be underestimated for the upper basalt layer and overestimated for the lower one. Nevertheless, this method allows one to track the vertical and lateral extents of different basalt units, as defined by their Ti content. In this context, the error of 1 wt% in the TiO_2 map (Lucey et al. 2000a) is not very significant.

Errors associated with the soil compositional data are 2 σ standard deviations calculated from the map readings; errors for the basalt compositional data are estimated based on the considerations listed above. The minimum basalt thickness is based on lower FeO reading and h/D_t ratio 0.1, the maximum basalt thickness is based on higher FeO reading and h/D_t ratio 0.14.

Our method is similar to the one used by Budney and Lucey (1998) in Mare Humorum. Their method differs from ours in that they used spectral endmembers as opposed to chemical ones, they used slightly different parameters for crater morphology, and they considered quantitatively radial zoning of ejecta originating from various depths.

Kodama and Yamaguchi (2003) studied eastern lunar maria, including M. Tranquillitatis and M. Fecunditatis, using Clementine false color images, iron and titanium data, albedo, UV/VIS ratio, and absorption near 1 μm and 2 μm. Their spectral parameters were read from soil. It is not clear whether their iron and titanium data represent soil or pure basalt compositions.

MARE TRANQUILLITATIS

Geological Setting

Mare Tranquillitatis (center: 7°N, 30°E; ~800 km in diameter) occupies a pre-Nectarian impact basin filled by ejecta from younger basins (Nectaris [oldest], Crisium, Serenitatis, and Imbrium [youngest]), which provide a brecciated, highlands-composition basement underlying the multiple basalt flows ranging in age from about 4.2 Gyr to

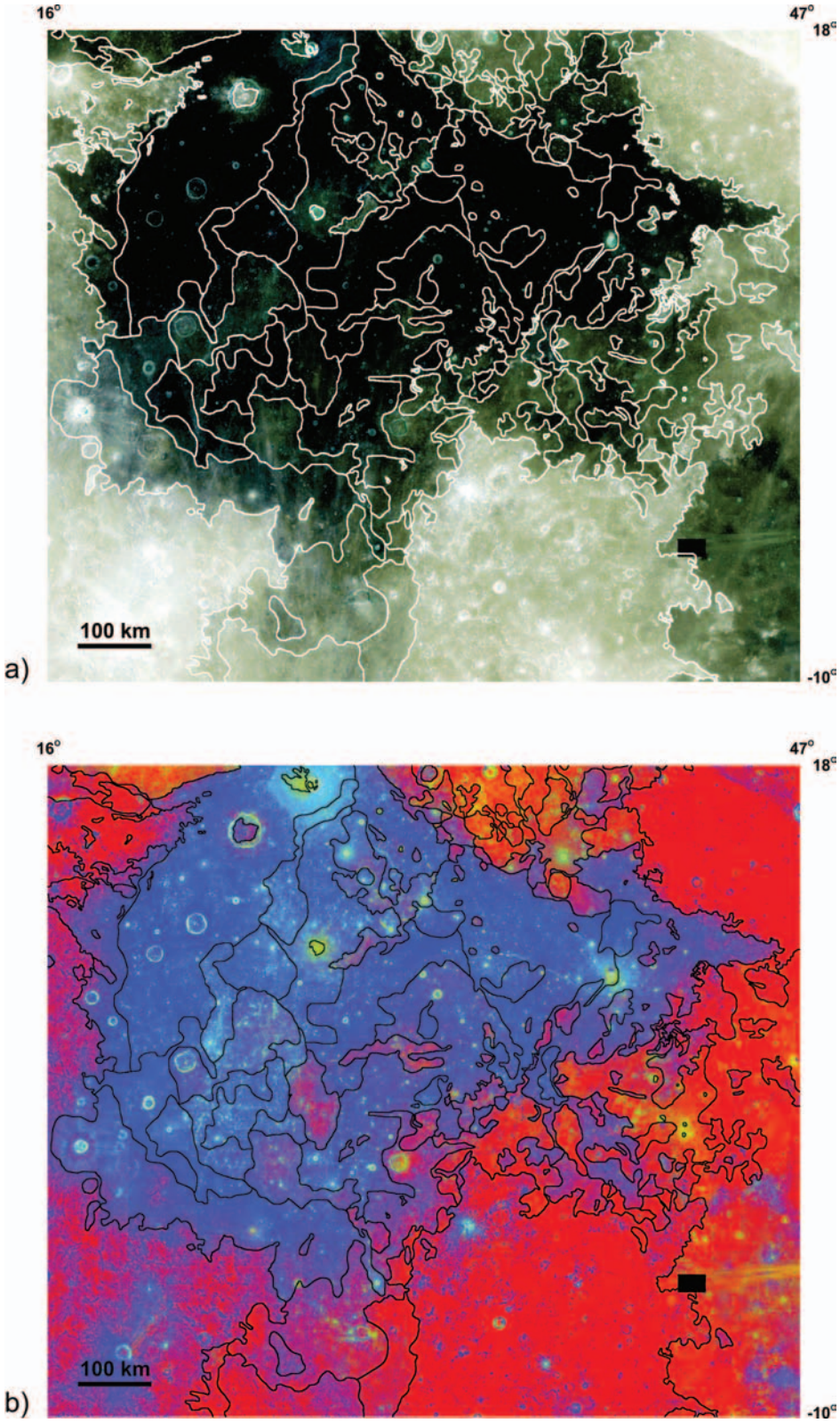

Fig. 3. Image mosaics and derived maps of Mare Tranquillitatis: a) "true" color image; b) false color image. The curved lines in each map are compositional unit boundaries. Mature highland material appears red in the false color image (b), excavated highland blue, low-Ti basalts orange, high-Ti basalts blue, and excavated basalts yellow to green. The maps are at the same scale as those in Figs. 5, 9, 10, and 13.

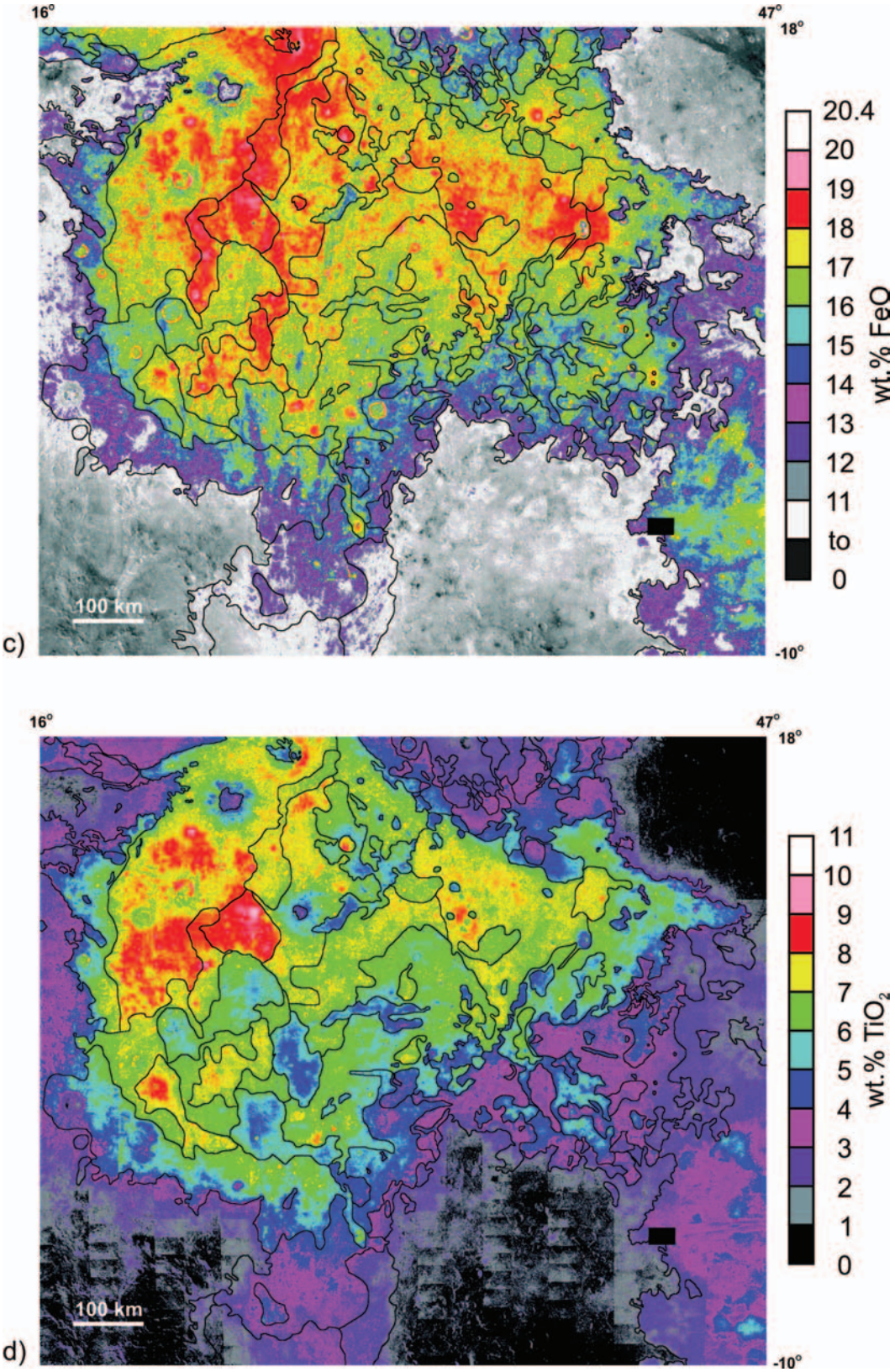

Fig. 3. *Continued.* Image mosaics and derived maps of Mare Tranquillitatis: c) FeO map; d) TiO_2 map. The curved lines in each map are compositional unit boundaries. Mature highland material appears red in the false color image (b), excavated highland blue, low-Ti basalts orange, high-Ti basalts blue, and excavated basalts yellow to green. The maps are at the same scale as those in Figs. 5, 9, 10, and 13.

3.4 Gyr based on crater counts (Wilhelms 1987; Hiesinger et al. 2000). Telescopic observation (Pieters 1978; Wilhelms 1987) and more detailed work based on Galileo data (Staid et al. 1996) distinguished Ti-rich basalts covering most of the mare and low to medium Ti-rich basalts occurring in marginal parts of the mare. Apollo 11 landed in the southern part of the mare within the high-Ti basalt units. Mare Tranquillitatis is a non-mascon basin, which indicates rather thin basalt infill (DeHon and Waskom 1976; Thurber and Solomon 1978).

Iron and Titanium Data

The Mare Tranquillitatis map shows a range of FeO (11–20 wt%) concentration (Fig. 3). The FeO concentration typically increases from mare margin toward center, but also varies significantly within the mare. The soil FeO composition in lunar maria has been interpreted primarily as a result of vertical mixing caused by impact excavation of highland basement beneath basalt (e.g., Rhodes 1977; Hörz 1978; Farrand 1988), and the FeO variation in mare soil has been viewed as an indication of basalt thickness variation. Recent studies based on Clementine multispectral data indicate, however, that lateral mixing is a dominant process along mare-highland contacts and may be important throughout whole maria (Mustard and Head 1996; Mustard et al. 1998; Li and Mustard 2000). In addition, the iron map displays a strong pattern of low-FeO ejecta rays from crater Theophilus located south of the mare. These ejecta appear to be a significant contribution to total highland contamination in the mare soil. The low FeO within the ejecta rays generally does not appear to be a maturity effect as the algorithms used for iron map calculation reduce most of the maturity effect (Lucey et al. 2000a) and the Theophilus rays in particular appear mature on the maturity index map of Lucey et al. (2000b). Significant highland content in Theophilus ejecta rays is consistent with the results of other studies that focused on bright rays of several craters (e.g., Pieters et al. 1985; Hawke et al. 1999). Rims of old craters with basement composition occur at several places throughout Mare Tranquillitatis (mainly in the south and east) and indicate basalts thinner than elsewhere in the mare and very uneven morphology of Tranquillitatis basement at a kilometer scale. Plinius on the NW margin of the mare is the most prominent example of a crater that excavated this basement and it displays ejecta with mixed FeO composition.

Titanium concentration in the Mare Tranquillitatis soil varies from less than 1 to 11 wt% TiO_2 (Fig. 3). This variation is caused in part by highland contamination (as indicated by the iron map) and also by variation in the basalt composition.

Collected data on FeO and TiO_2 compositions of soils and basalts for each unit illustrate both effects of contamination and basalt composition (Fig. 4). All the data in Fig. 4 are ordered according to basalt FeO content. Soil FeO content variation in a wide range of 11–18 wt% evidently reflects mixing between basalts and highland material. Basalts display a much narrower range of variation—within 16–19 wt% FeO. It is possible that this is a real variation in basalt compositions, but because the low iron values were typically recorded in marginal areas of the mare with higher levels of soil highland contamination, we might not fully avoid the effect of contamination in our determinations and we estimate greater error for these values. Soil TiO_2 content varies between 1 and 8 wt% following the same highland contamination trend as FeO. The TiO_2 data, however, vary significantly also between units with similar levels of the contamination (FeO) and indicate the existence of at least 2 to 3 basalt types in the mare with different TiO_2 contents. This variation in basalt composition stands out even more clearly from the basalt titanium data. TiO_2 in basalts varies from nearly 0 to almost 11 wt%. There is a clear difference between buried basalts that were resolved to be only Ti-poor and between basalts at the mare surface that range from Ti-poor to Ti-rich. Besides this distinction, the titanium data do not form any obvious compositional groups. Considering the estimated errors associated with our TiO_2 readings, we grouped the units arbitrarily every 2 wt% of TiO_2 and color-coded them in separate maps for surface and buried basalts (Fig. 5).

Basaltic Units

In agreement with previous work of Pieters (1978), Wilhelms (1987), Staid et al. (1996), and Kodama and Yamaguchi (2003), our maps show Ti-rich basalts covering most of Mare Tranquillitatis with Ti-poorer basalts in the north, east, and south. The buried units all appear to be low-Ti basalts. The HDWA basalts of Wilhelms (1987), interpreted to contain 5–10 wt% TiO_2 (Pieters 1978), cover about half of the mare and fit almost exactly our blue units (>8–11 wt% TiO_2, see Fig. 5). The HDWA basalt as mapped by Pieters (1978) also includes most of our green units (>6–8 wt% TiO_2) (Fig. 6). The Fecunditatis type mIG basalts (0–4 wt% TiO_2) (Pieters 1978; Wilhelms 1987) in the north and east correspond to our green and yellow units (>6–8 and >4–6 wt% TiO_2). The hDW unit (3–6 wt% TiO_2) (Pieters 1978) in the southeast matches our green units. The Nectaris type, 0–4 wt% TiO_2, mBG basalt (Pieters 1978) in the south corresponds to our yellow and orange units (>4–6 and >2–4 wt% TiO_2).

The very high titanium unit $T_{vh\text{-}A}$ of Staid et al. (1996) in the west to southwest corresponds entirely to our blue units (Fig. 6). The very high titanium units $T_{vh\text{-}B}$ (Staid et al. 1996) include the rest of our blue units and also most of our green units. The high titanium units T_h are similar to our green units, which are the Ti-poorer members of the green class (>6–8 wt% TiO_2). The low titanium units T_l are clearly spatially related to our yellow units but the match is not very good. In the southeast the T_l includes also some of our green units and in the north it includes our yellow, green, and even blue units.

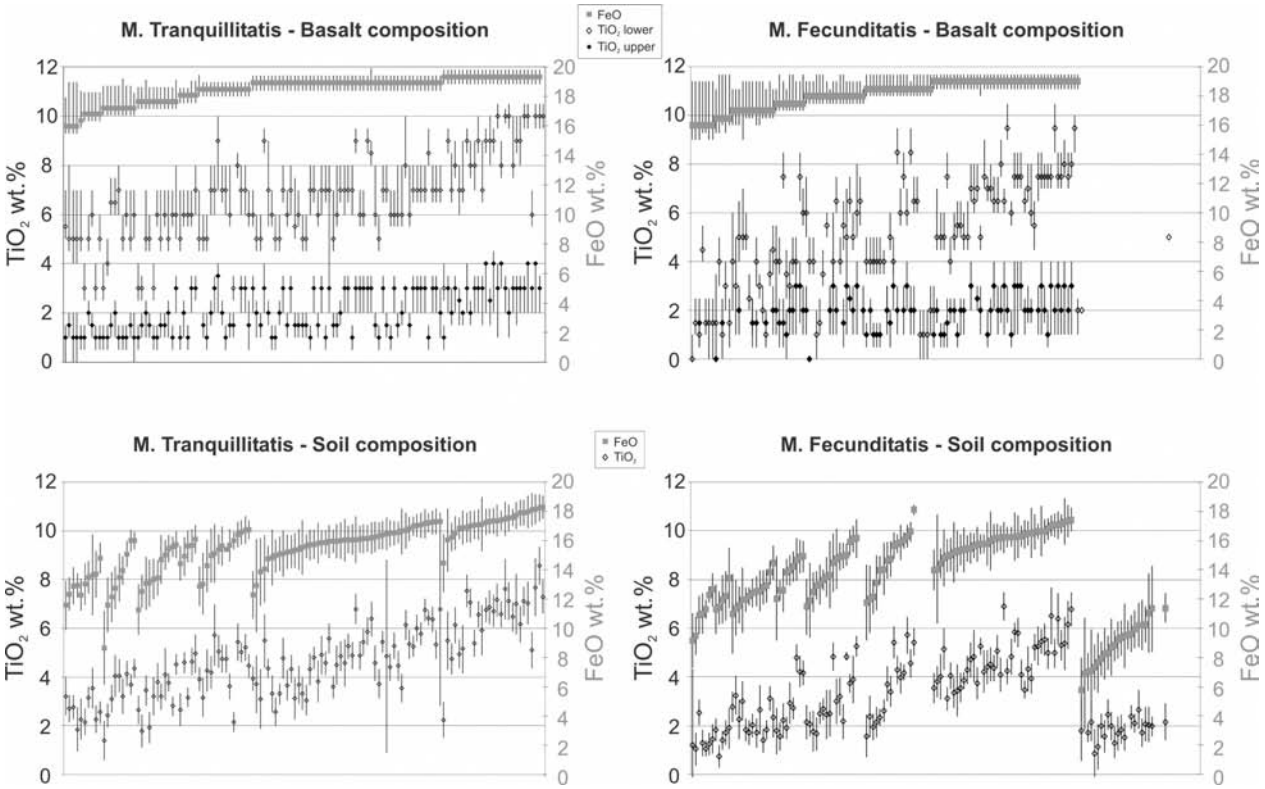

Fig. 4. Geochemical data for units in the studied maria. Both soil and basalt data for respective maria are ordered according to increasing FeO in basalt. Some units in Mare Fecunditatis have soils heavily contaminated with highland material (low FeO), and basalt composition for these units could not be determined. Uncertainties in soil data are 2 σ calculated from the sampled pixels of the maps. Uncertainties in basalt data are estimated at 2 σ level.

Definition of some units, such as the unit T_h mapped around Plinius and Maskelyne and $T_{vh\text{-}B}$ around MacLear, clearly reflects contamination of soil with the underlying low-Ti basalt indicated in our map. In our opinion, these basalt units represent the same basalt at the surface as the surrounding units.

Overall, our units match well the Pieters (1978), Wilhelms (1987), and Staid et al. (1996) spectrally defined units. Thanks to better spatial resolution of the original data, our maps resolve the units in greater detail. We also associate our units with higher titanium content. This difference is not surprising considering the mapping methodology we used. The definition of the spectral units is based on spectral signal derived from mare soil, which reflects contamination with titanium poor highland material and mixing of different basalts. Our units are based on direct observation of basalt composition in small craters. This approach allows more accurate definition of the basalt composition for each unit and also better spatial definition of each basalt unit in a situation when the top unit is gradually thinning.

Comparison of our units with those (Tr1 through 5) defined by Kodama and Yamaguchi (2003) is not straightforward. Tr1 corresponds compositionally to our orange, but spatially overlaps with our orange, partly yellow and even blue units in the west. Tr2 spatially overlaps with some of our green but it has 2 wt% higher TiO_2 content. Tr3 spatially overlaps with ~50 % of our blue and ~50 % of green units. Its TiO_2 content is ~2 wt% higher than for our blue units. Tr4 overlaps with our blue units in the west and southwest. Its TiO_2 content is ~3.5 wt% higher, however. Tr5 overlaps with our yellow and green units in the east and north, and compositionally corresponds to yellow units. These differences can be partly attributed to the use of soil characteristics in the classification methodology of Kodama and Yamaguchi (2003).

Basalt Thickness

The map of total basalt thickness documents uneven morphology of the mare basement at a basin scale (Fig. 7). Since the data points with estimated basalt thickness were sparsely distributed over the map, the contours could be drawn in various ways. Our contouring is based on an assumption that the morphological features of the mare basement are all of impact origin and therefore tend to be circular. Our data show that the eastern part of Mare Tranquillitatis is relatively shallow: 50–400 m deep with a few deeper pockets. The western part of the mare is much

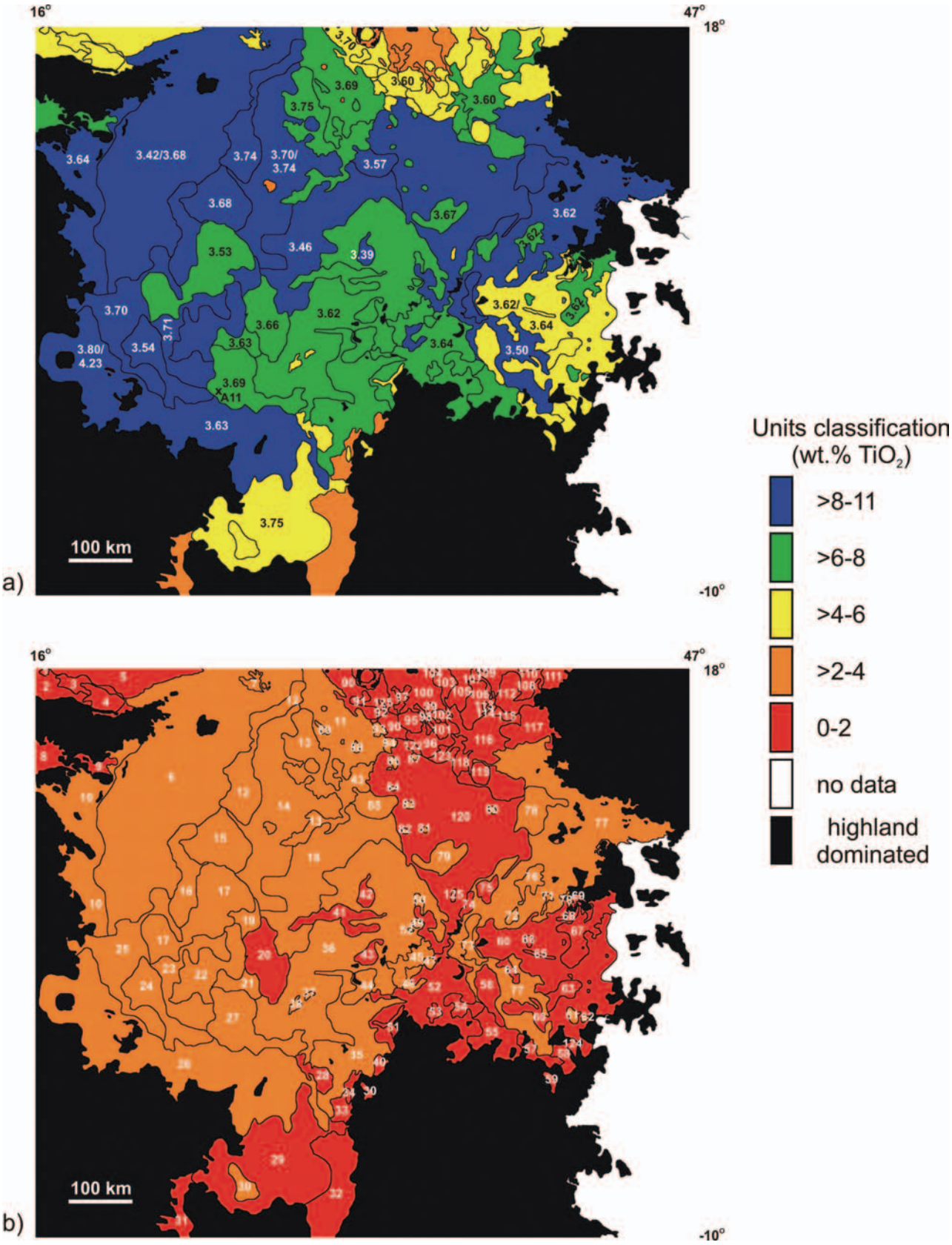

Fig. 5. Geologic map of Mare Tranquillitatis: a) surface units with age data of Hiesinger et al. (2000) in Ga; b) buried basalt with unit identification numbers. A11 = Apollo 11 landing site.

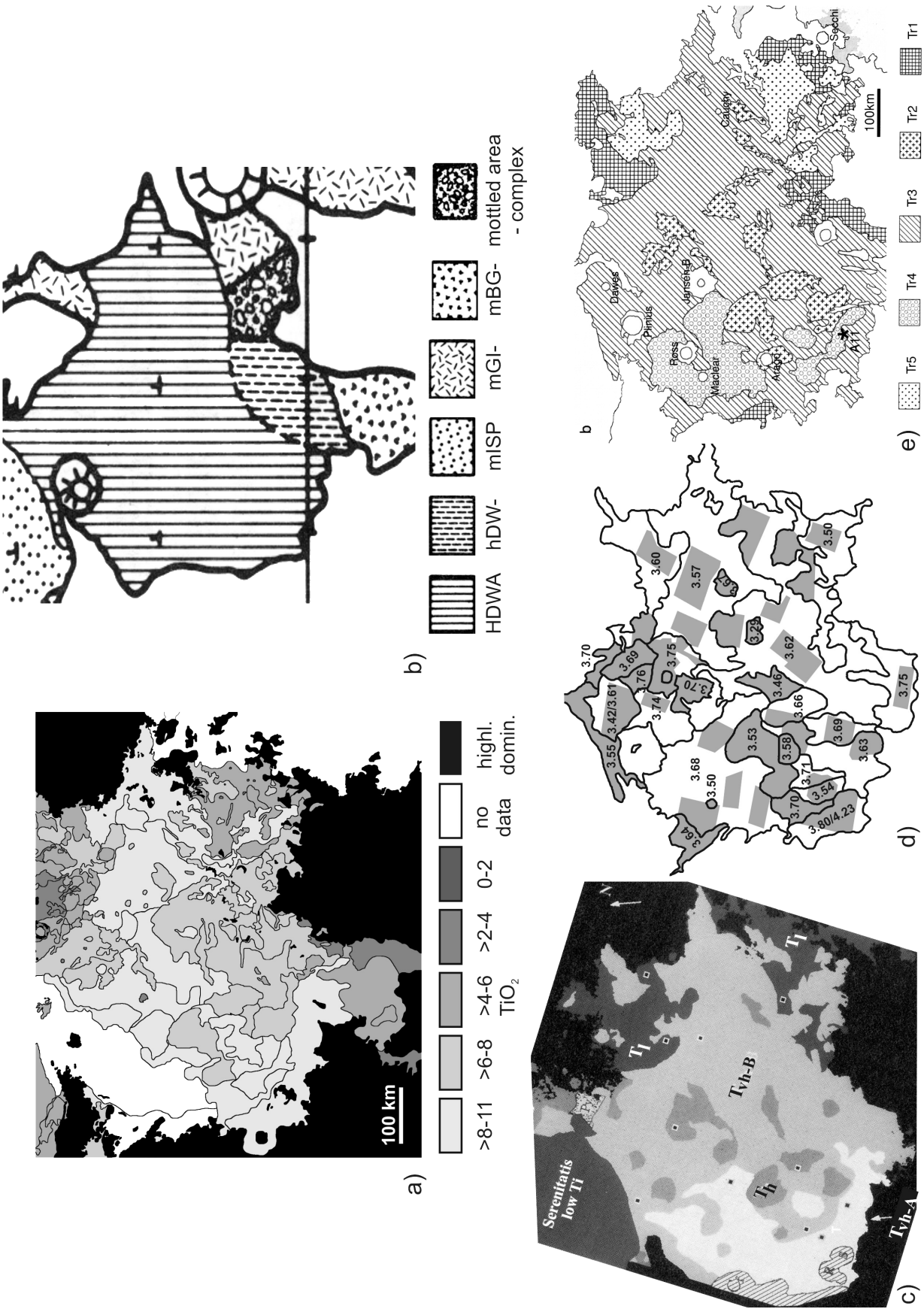

Fig. 6. Comparison of geologic maps of Mare Tranquillitatis: a) this study; b) Pieters (1978); c) Staid et al. (1996); d) Hiesinger et al. (2000), redrawn after original, each unit displays an age in Ga, shaded fields are the areas where ages were measured; e) Kodama and Yamaguchi (2003). The maps are at the same scale as those in Fig. 11.

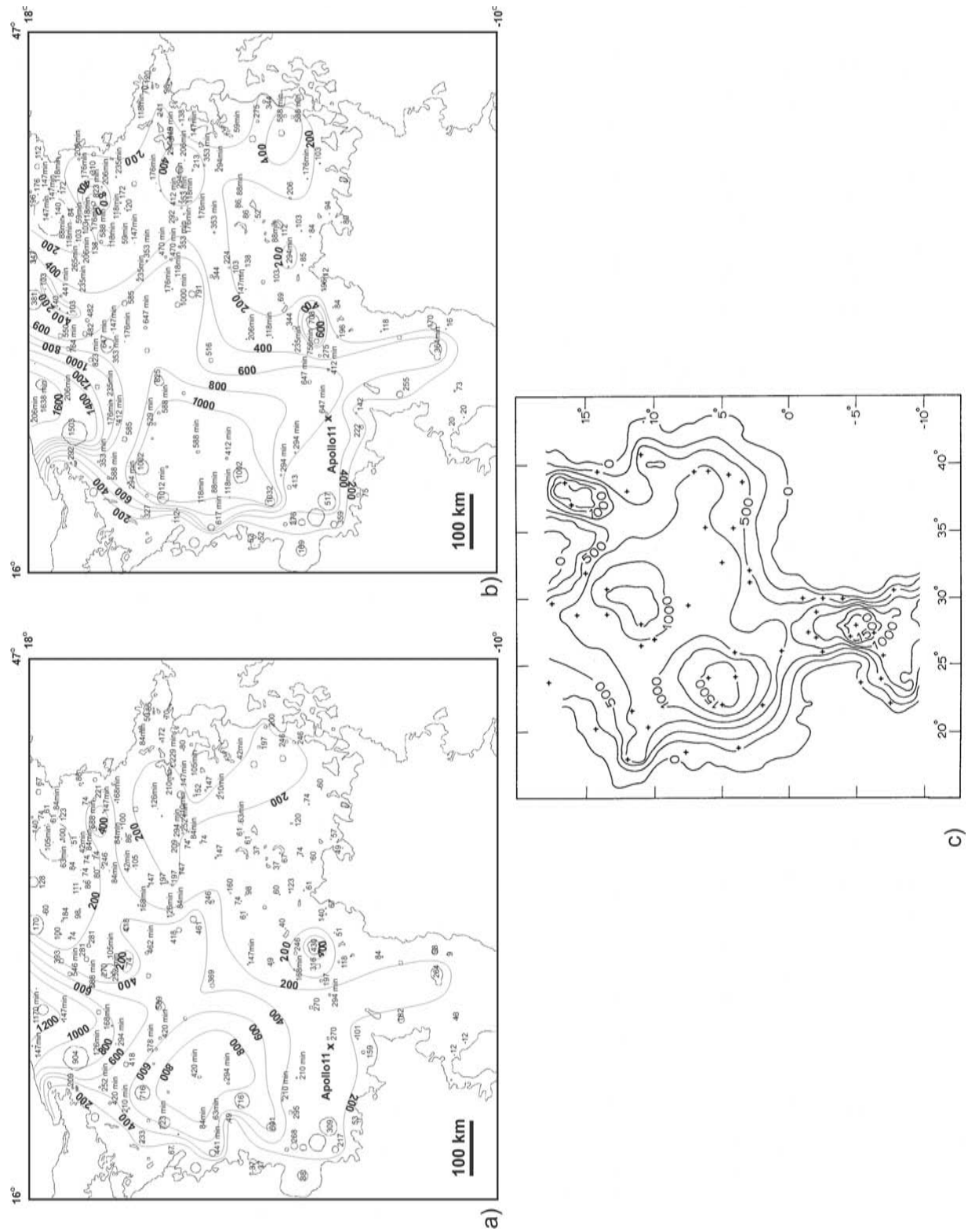

Fig. 7. Basalt thickness maps of Mare Tranquillitatis and comparison with previous work: a) this study, maximum estimate based on $h/D_t = 0.14$ and higher FeO values for crater ejecta; b) this study, minimum estimate based on $h/D_t = 0.1$ and lower FeO values for crater ejecta; c) DeHon (1974). The thickness data, such as "290 min," indicate that the particular crater excavated only basalt and the thickness estimate is, thus, at least the crater excavation depth. All data are in meters. The maps are at the same scale as those in Fig. 12.

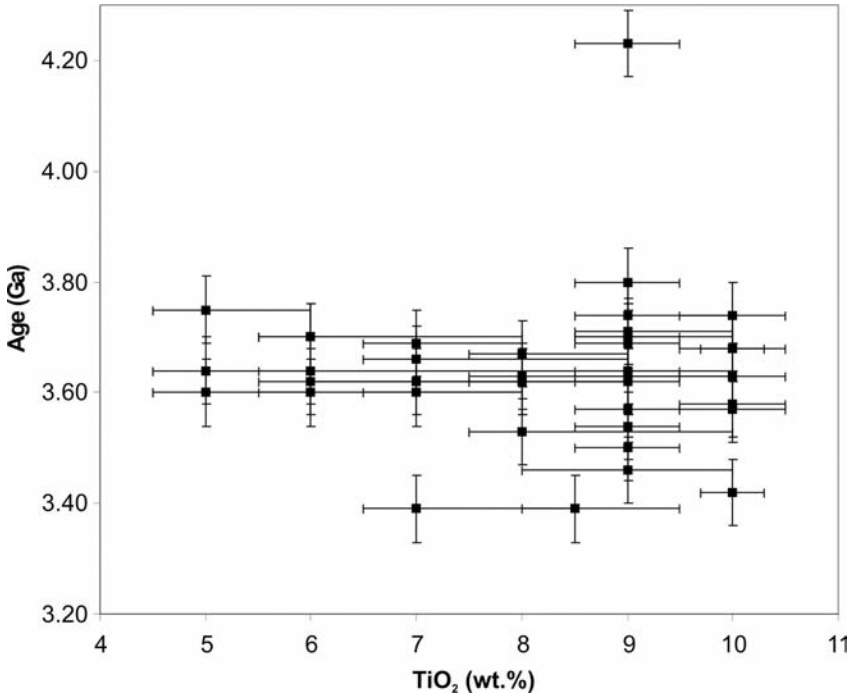

Fig. 8. Distribution of Mare Tranquillitatis basalts with various titanium content in time. The titanium data are from this work and the age data are from Hiesinger et al. (2000).

deeper, 200–1000 m, and in the NW (near M. Serenitatis) the thickness reaches 1200–1600 m.

DeHon (1974) previously derived basalt thickness in the mare from partially flooded craters (Fig. 7). He assumed height of crater rim based on crater diameter and he measured height of the rim above basalt flow. The difference between these two heights corresponded to basalt thickness which was on average 500–600 m and at some places over ~1500 m. Hörz (1978) modified this method by accounting for the fact that many of the craters were degraded at the time of flooding and the height of crater walls was about a half of the original height. Hörz (1978) lowered DeHon's (1974) estimate by a factor of 2. On the other hand, at least some of the craters used in this method lay on preexisting lava flows and not on basement (Hörz 1978). Therefore, Hörz (1978) may have somewhat underestimated the thickness.

Head (1982) argued that by using an average crater rim height and not accounting for the height variation along rims of individual craters the methods of DeHon (1974) and Hörz (1978) underestimate basalt thickness.

Our thickness estimates fall within the range previously presented by DeHon and Hörz. The only major difference occurs in the northwestern area of the mare close to Mare Serenitatis. Our maps indicate much greater thickness there than the maps of DeHon and Hörz.

Thurber and Solomon (1978) modeled Apollo gravity data and, for non-mascon Mare Tranquillitatis, indicated basalt thickness of average ~500 m and locally over 1000 m. These thicknesses are an underestimate because the used model did not consider mare subsidence (Thurber and Solomon 1978). A local gravity high in the western Mare Tranquillitatis (Sjogren et al. 1973; Lemoine et al. 1997; Konopliv et al. 2001) correlates with the thick basalt in our and DeHon's maps and relatively lower gravity in the east of the mare corresponds to thin basalts in both maps. The basalt accumulation shown by DeHon in the north-central part of the mare is not supported by gravity data. Our map fits the gravity data better in this area. DeHon's map, on the other hand, matches better intermediate gravity near the boundary with Mare Serenitatis.

Stratigraphy and Magmatic History

The observed spatial distribution and stratigraphic relationships of the mapped units suggest that magmatism in the mare started with voluminous low-Ti basalts and evolved toward higher-Ti. Although the medium- to high-Ti basalts extend across most of the mare they appear only meters to a few tens of meters thick and their thickness varies widely over short distances. The thicknesses of the top layers are consistent with thickness estimates for individual lava flows based on photogeologic evaluations (e.g., Howard et al. 1972; Schaber et al. 1976; Gifford and El-Baz 1981) and crater size-frequency distributions (Hiesinger et al. 2002). We also infer low-Ti composition for buried basalt beneath the Apollo 11 landing site. However, Apollo 11 did not sample any low-Ti basalt. Possible explanations of this discrepancy within the context of our interpretation include: 1) regolith at the landing

site is primarily derived from the top basalts; 2) the estimates of TiO_2 composition of the buried basalts is significantly affected by the topographic error; 3) the material exposed at craters that excavated the buried basalt contains much less mixed-in top basalt than we inferred and, therefore, reveals more pristine titanium content; 4) our interpretation simplifies the stratigraphy into two basalt layers although, in reality, the mare fill probably consists of multiple layers with an overall gradient in titanium content.

We were able to associate some of our surface units in Mare Tranquillitatis with age data of Hiesinger et al. (2000). All of the surface basalt compositional groups span a wide range of ages; some of the high-Ti basalts show the oldest ages in the mare (Fig. 8). Therefore, the upper part of the stratigraphic column of basalts in Mare Tranquillitatis must consist of overlapping flows with alternating medium to high TiO_2 contents. We saw indication of such stratigraphy in units #17 and #20 in Lamont area where very small craters of just a few hundred meters in diameter appeared to excavate high-Ti basalt from beneath medium-Ti basalt. But because each of the craters was represented by only one or two pixels in the map, we were not sure that we could trust such "anomalous" results. We did not resolve any obvious lava sources in Mare Tranquillitatis. Only Cauchy rille appeared to be related to emplacement of the large high-Ti unit #120.

The observed trend of increasing Ti content with time within Mare Tranquillitatis basalts is at odds with the opposite trend in global lunar sample collection (e.g., Nyquist and Shih 1992). This can be explained by sparse sampling of the lunar surface. Detailed comparison of iron and titanium content and crater-count-based ages of surface lava units in several maria showed no trend (Hiesinger et al. 1998; Hiesinger et al. 2001). Staid et al. (1996) identified a general trend in Mare Tranquillitatis lavas from low- to high-Ti (consistent with our observation) based on stratigraphic observation in several impact craters. Both our and Staid et al. (1996) studies rely on observation of buried basalts which are inaccessible for crater-count dating. Kodama and Yamaguchi (2003) observed similar stratigraphic trend, but noticed an example of the reversed low-over-high-Ti basalt order in the northeast. Jerde et al. (1994), recognized three magmatic events within the Apollo 11 high-Ti basalts. The oldest B2-D basalts (low-K, 8.4–8.9 wt% TiO_2) formed from low-K source at ~3.85 Ga and the younger B3-B1 basalts (low-K, 10.0–10.3 wt% TiO_2), derived from the same source, formed at 3.67–3.71 Ga. The youngest A basalts (high-K, 11.0 wt% TiO_2) formed from a different source at ~3.59 Ga (Jerde et al. 1994). Our data indicate that the oldest high-Ti basalts (Fig. 8) contain 9 wt% TiO_2 and are 3.8–4.23 Ga old, and the basalts with 9–10 wt% TiO_2 are younger, which is consistent with Jerde et al. (1994). Our data do not show any basalt with 11 wt% TiO_2 at ~3.59 Ga because our determined compositions are averages for each unit and/or because we may have slightly underestimated the titanium content.

MARE FECUNDITATIS

Geological Setting

Mare Fecunditatis (center: 4°S, 51°E; ~600 km diameter) occupies a pre-Nectarian impact basin filled by ejecta from Nectaris (oldest), Crisium, and Imbrium (youngest) basins (Wilhelms 1987). This brecciated, highlands-composition, basement is covered by basalt lavas ranging from 3.7 to 3.15 Ga radiometric age (Basaltic Volcanism Study Project 1981; Cohen et al. 2001). Telescopic observations discovered mainly low-Ti basalt with a small wedge of medium Ti-rich basalt in the north. An area in the south of the mare remained unclassified (Pieters 1978; Wilhelms 1987). Farrand (1988) studied Mare Fecunditatis at a higher spatial resolution and distinguished four basalt units based on Earth-based telescope albedo, multispectral and Apollo X-ray Al/Si and Mg/Si data. All the units can be, however, chemically characterized as an average Apollo 12 low-Ti basalt or average high-alumina basalt with various admixtures of highland component (Farrand 1988). Mare Fecunditatis has been sampled by Luna 16 at the southern tip of the medium Ti-rich basalt wedge. The collected basalts are aluminous, low-Ti with average TiO_2 content around 5.1 wt% (Taylor et al. 1991). Mare Fecunditatis is a non-mascon basin with rather thin basalt infill (DeHon and Waskom 1976; Thurber and Solomon 1978).

Iron and Titanium Data

The FeO map of Mare Fecunditatis (Fig. 9) shows similar variations in soil iron content as the map of Mare Tranquillitatis. Soil of Mare Fecunditatis is significantly more contaminated by highland component. Much of this contamination comes from ejecta of two large craters—Taruntius in the northwest and Langrenus in the southeast. In other parts of the mare the contamination is probably controlled by local impact excavation of the basement. Many old crater rims with highland FeO content stand up from the basalt flows as in the eastern Mare Tranquillitatis.

The TiO_2 map (Fig. 9) partly follows the pattern of highland contamination as shown in the FeO map, but also displays distinct patches of medium to high Ti soil on a generally low Ti background.

Collected data on FeO and TiO_2 compositions of soils and basalts for each mapped unit display quite similar relationships and patterns as the data from Mare Tranquillitatis (Fig. 4). Soil composition ranges from 6 to 18 wt% FeO and from 1 to 7 wt% TiO_2. The titanium and iron data follow the contamination mixing trend between low-Fe-Ti basement and high-Fe-Ti basalts. The titatium data also display variations that suggest sampling of at least two basalt types with different titanium content. Basalt FeO concentration varies between 16 and 19 wt%. The lower

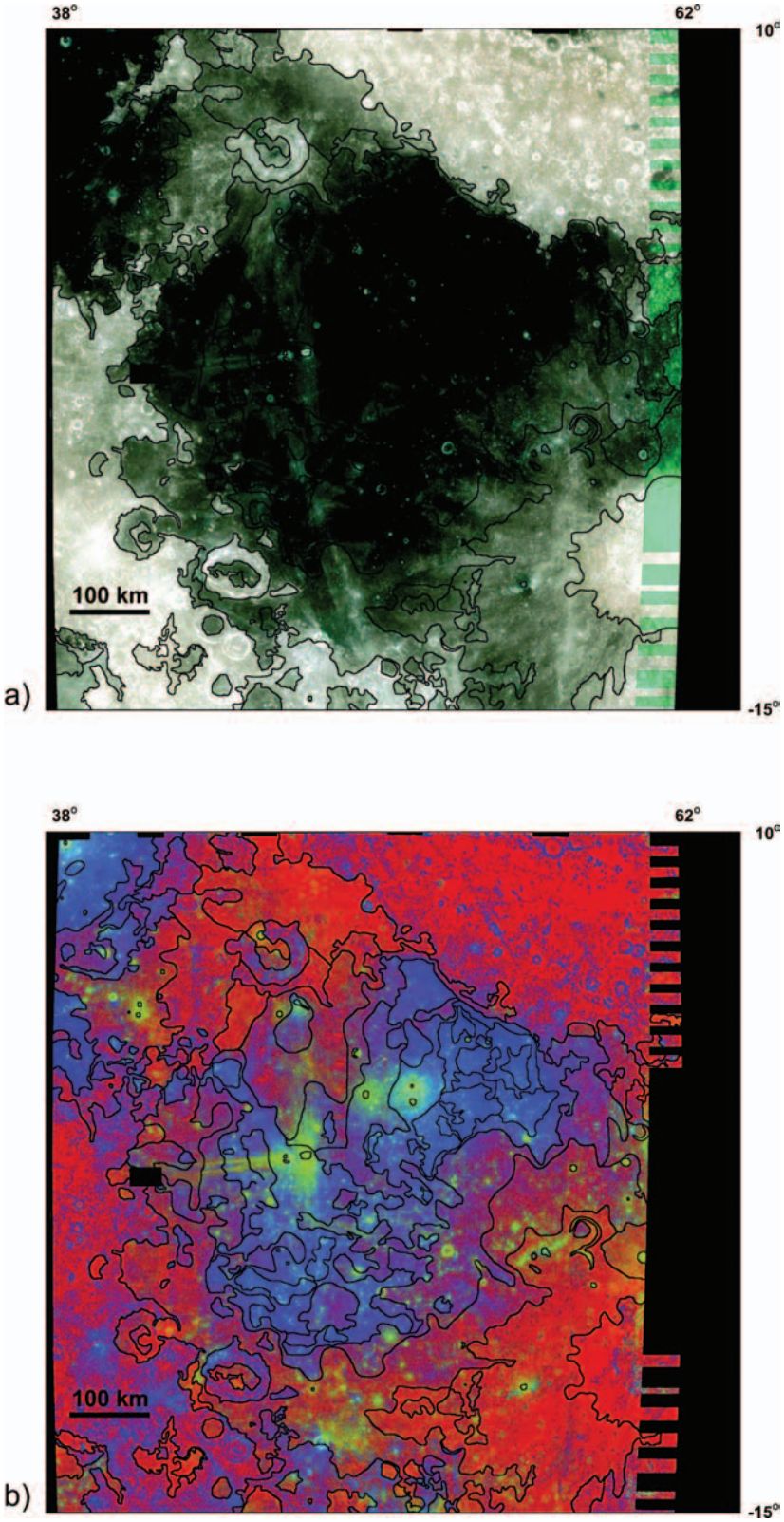

Fig. 9. Image mosaics and derived maps of Mare Fecunditatis: a) "true" color image; b) false color image. The curved lines in each map are compositional unit boundaries. Mature highland material appears red in the false color image (b), excavated highland blue, low-Ti basalts orange, high-Ti basalts blue, and excavated basalts yellow to green.

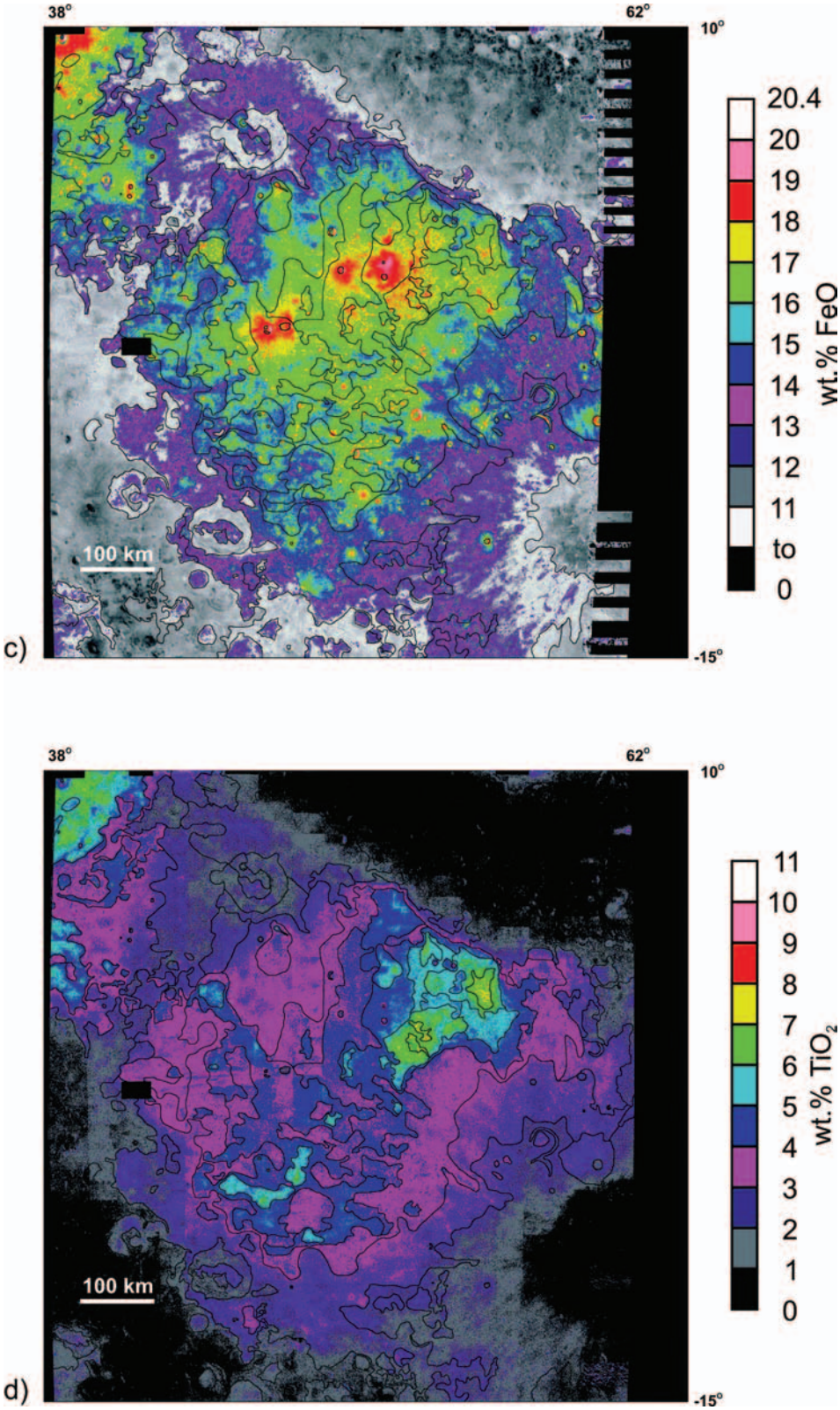

Fig. 9. *Continued*. Image mosaics and derived maps of Mare Fecunditatis: c) FeO map; d) TiO_2 map. The curved lines in each map are compositional unit boundaries. Mature highland material appears red in the false color image (b), excavated highland blue, low-Ti basalts orange, high-Ti basalts blue, and excavated basalts yellow to green.

values typically come from highly contaminated units and have, therefore, greater error. Basalt TiO_2 data clearly distinguish low Ti basalts from medium to high Ti basalts. All buried basalts fall into the low-Ti category. The topmost basalts show a wide range of compositions; many of them are low Ti basalts. We classified the basalts into groups every 2 wt% TiO_2 and represented them in maps as in Mare Tranquillitatis (Fig. 10).

Basaltic Units

Basalts exposed at the surface of Mare Fecunditatis belong mostly to low to medium Ti types (0–6 wt% TiO_2). High-Ti basalts crop out in central to north central areas of the mare and their extent is much smaller than in Mare Tranquillitatis. The buried basalts are all low-Ti (Fig. 10). The wedge of green (>6–8 wt% TiO_2) and blue (>8–11 wt% TiO_2) units in the north corresponds well to the hDW unit (3–6 wt% TiO_2) of Pieters (1978) and hDWA of Wilhelms (1987). Most of the mare mapped as mGI (0–4 wt% TiO_2) unit (Pieters 1978; Wilhelms 1987) is in our maps covered by variety of basalts ranging between 2 and 8 wt% TiO_2. In the area that Pieters and Wilhelms called complex and left unclassified, we mapped whole range of basalt types including a few blue units (Fig. 11).

Farrand (1988) divided Mare Fecunditatis in units based on cluster analysis of Apollo X-ray Al/Si data and Earth-based spectral data (560 nm, 380/560 nm, and 850/380 nm), which he used as a proxy of albedo, age, and titanium content respectively (Fig. 11). Farrand's multispectral and X-ray data had two orders of magnitude lower spatial resolution than our data. His maps reveal greater heterogeneity of the mare basalts than the spectral units of Pieters (1978) and Wilhelms (1987). His first map excluded the effect of Al/Si data, the second map included Al/Si data. Farrand's a3 and b3 units appear to reflect mainly highland contamination caused by Taruntius and Langrenus ejecta. They may also partly reflect 2–4 wt% TiO_2 basalts of our orange units. The a2 and b2 units appear to correspond to our green and blue units in the north, but they do not occur elsewhere in the mare where our maps show the same basalt types. The a1 and b1 units somewhat resemble our field of yellow and green units in the mare. Other units on Farrand's map do not show clear relationship to our map.

The units Fc1 through 4 defined by Kodama and Yamaguchi (2003) are compositionally and spatially more similar to ours then in M. Tranquillitatis. Fc1 and Fc2 correspond compositionally and spatially to our orange and red units, respectively. The greater extend of Fc2 can be attributed to an interpretation ambiguity due to the extensive Langrenus ejecta. Fc3 corresponds compositionally and spatially to our green and blue units. Fc4 corresponds compositionally to our yellow units, but also overlaps some of our green and orange units.

Jakeš et al. (1972) distinguished two types of basaltic glasses in Luna 16 regolith based on their Al, Fe, and Ca content. The most abundant type A has much lower titanium content (2.6 wt% TiO_2) than the type B (7.0 wt% TiO_2). According to our geologic map, both compositions would be expected and the Luna 16 landing site (Fig. 10).

Basalt Thickness

The basalt thickness in Mare Fecunditatis ranges from essentially zero on mare margins to more than 1 km. Major accumulation of basalt occurs in central western part of the mare, with a maximum around Messier crater. Another major accumulation occurs in the eastern part of the mare between craters Langrenus and Webb, and yet another one around Messier G. There are relatively thin basalts right in the central part of the mare. Numerous small craters NE of Coglenius near the 200 m contour line excavate only basalt and indicate the thickness of at least 150–200 m (Fig. 12 and 13).

DeHon and Waskom (1976) mapped basalt thickness in Mare Fecunditatis using the method of DeHon (1974) and indicated average thickness of ~500 m and local accumulations up to 1500-m thick. Hörz (1978) then lowered their estimate by half (Fig. 12). As with Mare Tranquillitatis, both studies may have underestimated the thickness (Head 1982).

Farrand (1988) estimated basalt thickness from Al/Si data which served as an indicator of highland contamination. He assumed that the contamination was of local origin via impact gardening and the degree of contamination in the regolith was related to basalt thickness.

Our map roughly corresponds to previous maps in terms of identification of major basalt accumulations and the thin zone crossing the mare south of crater Messier from east to west. The previous maps, however, ignored basalts surrounding crater Taruntius. Our map indicates tens to over 100 m of basalts north and west of the crater. Quantitatively, our estimates fall within the range of DeHon and Waskom (1976) and Hörz (1978), but exceed Farrand's (1988) estimate by a factor of 8. Farrand himself thought that the true thickness is greater and considered his results a minimum limit. Farrand pointed out that his method assumed all contamination to come from a basement, whereas, in fact, some of the contamination came from old buried regolith. Therefore, his method underestimates the true thickness. It is not clear to us why our results do not reflect the same effect although we used a similar approach with different chemical tracer. The discrepancy between our and Farrand's estimates can also be documented at Messier and Messier A craters where, based on Al/Si data, Farrand suggested that the crater ejecta were slightly contaminated with basement, whereas our iron map shows only pure basaltic values.

The new basalt thickness estimates are in agreement with Mare Fecunditatis being a non-mascon basin. Thurber and Solomon (1978) modeled Apollo gravity data and, for non-

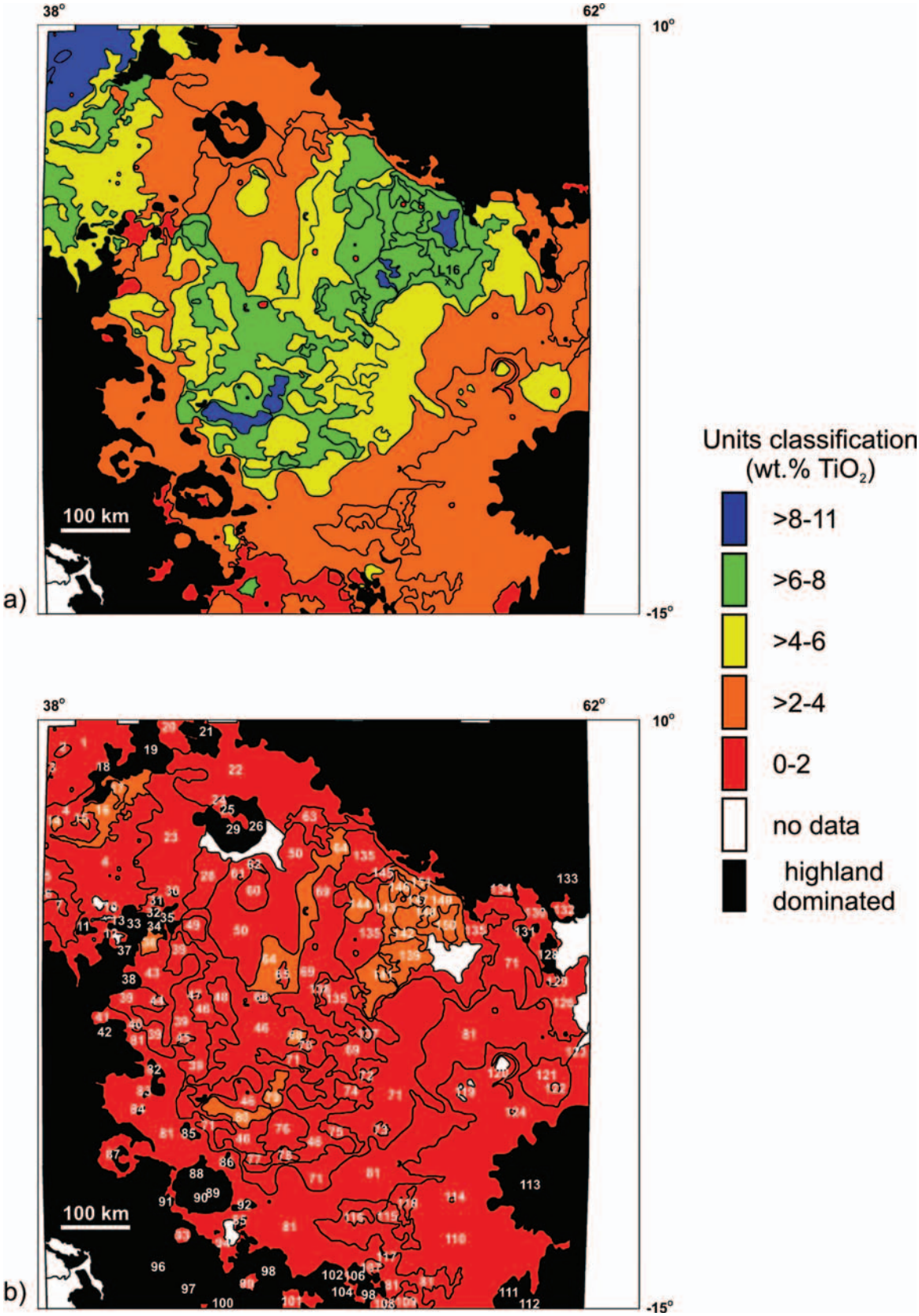

Fig. 10. Geologic map of Mare Fecunditatis: a) surface units; b) buried basalt with unit identification numbers. L16 = Luna 16 landing site.

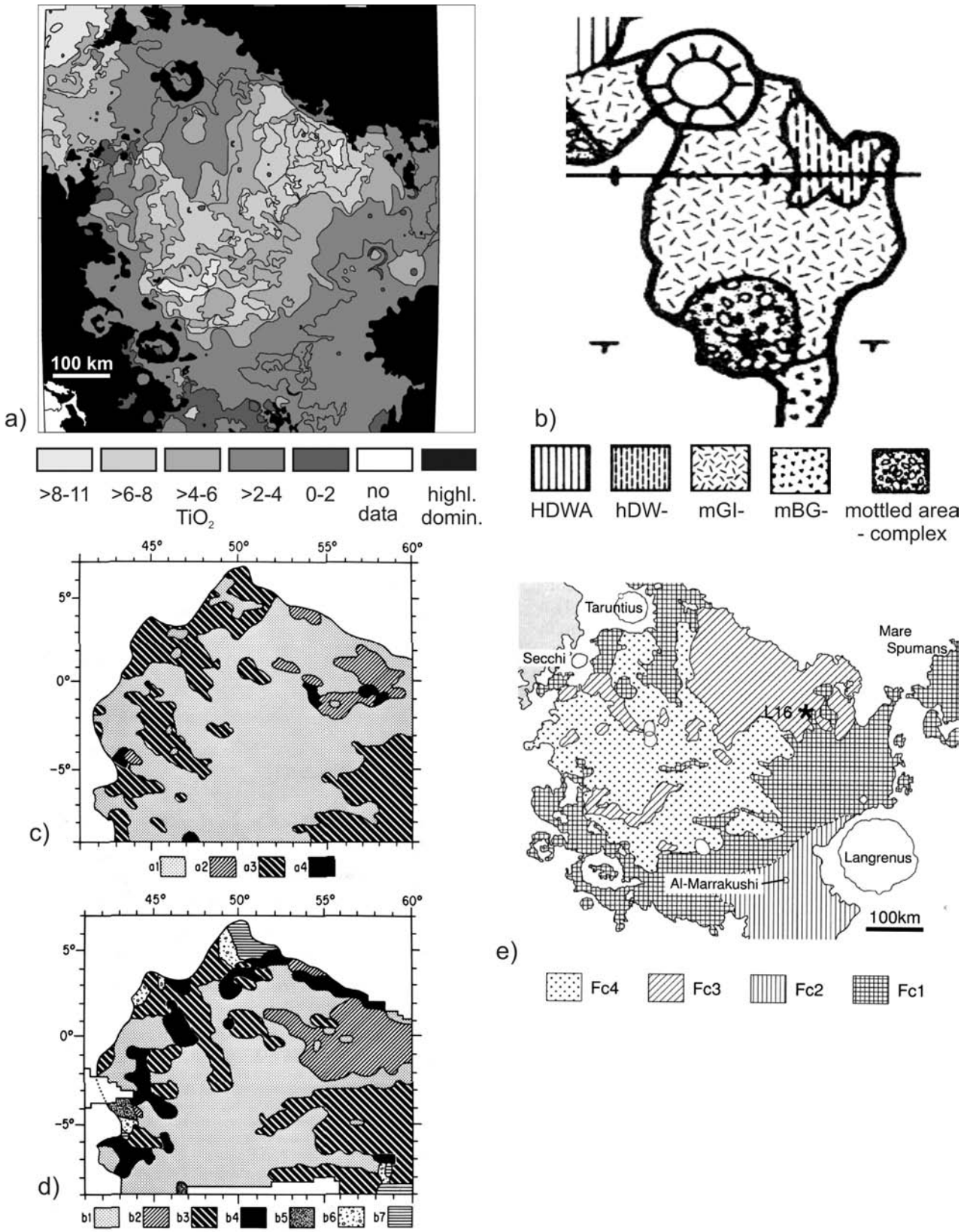

Fig. 11. Comparison of geologic maps of Mare Fecunditatis: a) this study; b) Pieters (1978); c) Farrand (1988), without Al/Si data; d) Farrand (1988), with Al/Si data; e) Kodama and Yamaguchi (2003).

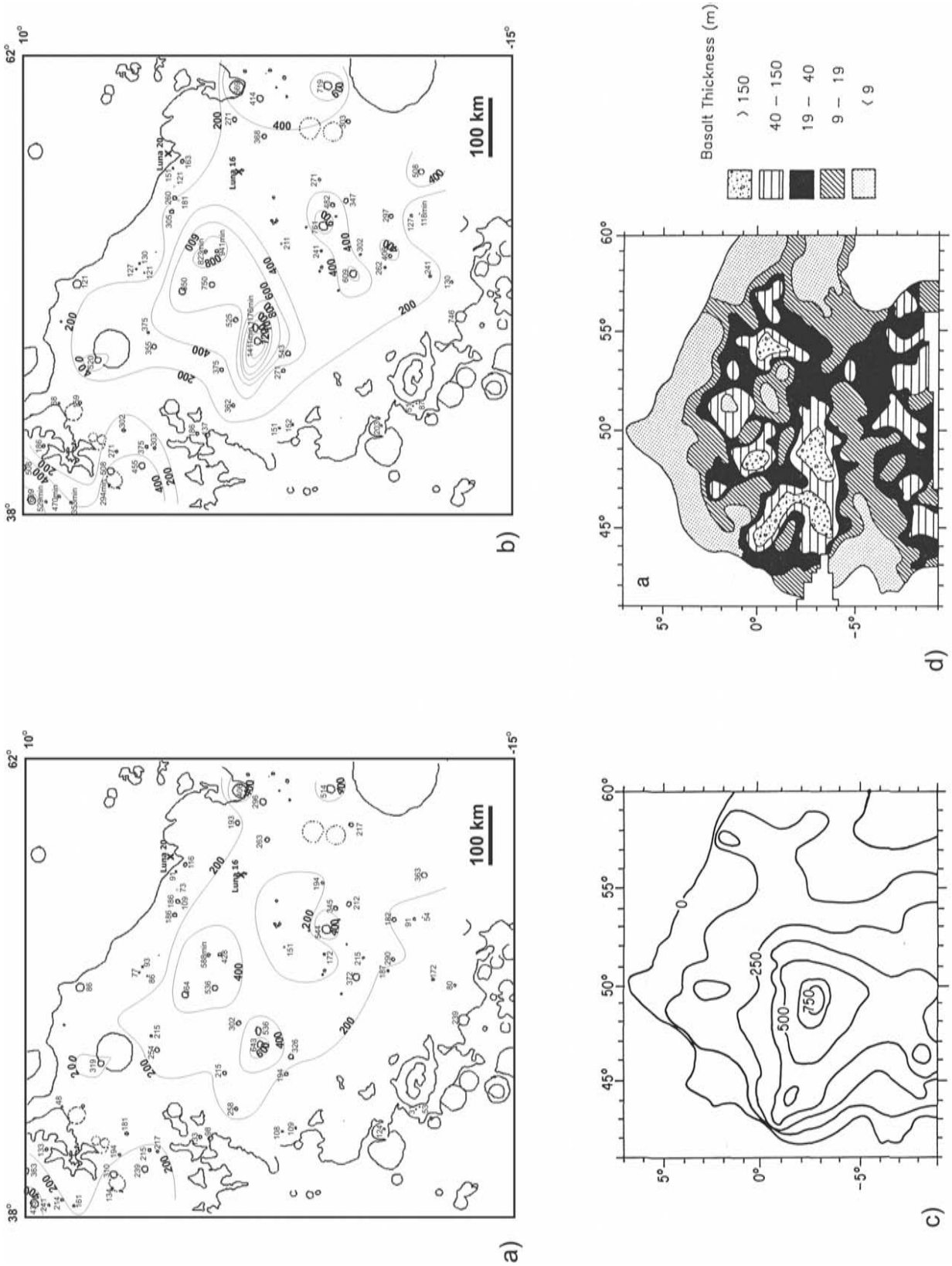

Fig. 12. Basalt thickness maps of Mare Fecunditatis and comparison to previous work: a) this study, maximum estimate based on $h/D_t = 0.14$ and higher FeO values for crater ejecta; b) this study, minimum estimate based on $h/D_t = 0.1$ and lower FeO values for crater ejecta; c) Hörz (1978) in Farrand (1988); d) Farrand (1988). The thickness data, such as "290 min," indicate that the particular crater excavated only basalt and the thickness estimate is, thus, at least the crater excavation depth. All data are in meters.

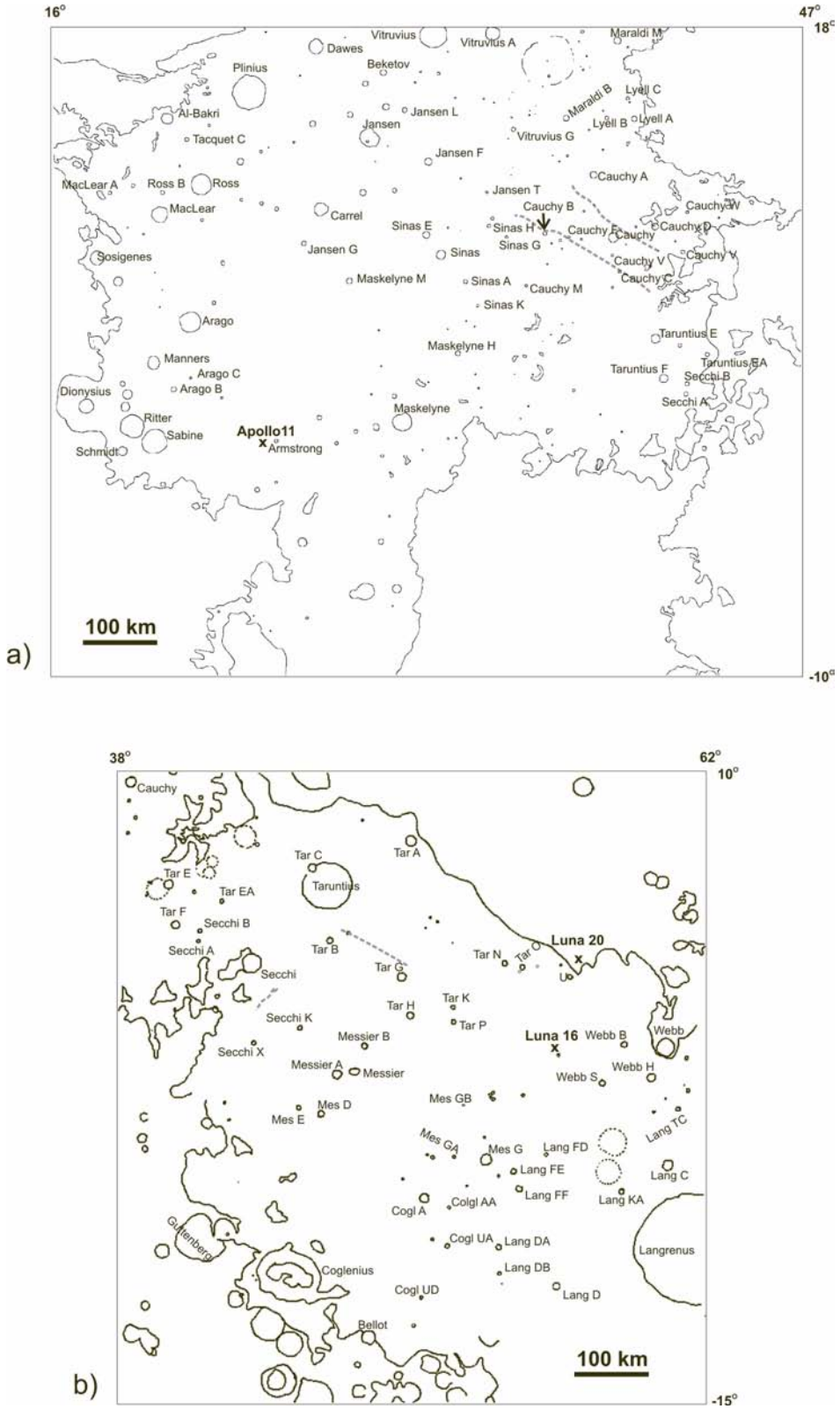

Fig. 13. Maps with names of craters used for basalt thickness estimates and other topographic features discussed in the text: a) Mare Tranquillitatis; b) Mare Fecunditatis. The dashed lines in Mare Tranquillitatis are Cauchy Rilles. The dashed lines in Mare Fecunditatis are possible lava sources.

mascon Mare Fecunditatis, indicated lower bound basalt thickness of on average ~500 m and locally over 1000 m. Low altitude gravity data show a broad gravity high in the west central part of the mare (Sjogren et al. 1973; Lemoine et al. 1997; Konopliv et al. 2001) consistent with local basalt accumulation, as indicated in our map.

Stratigraphy and Magmatic History

As in Mare Tranquillitatis, the top basalts are only meters to tens of meters thick and, therefore, the buried low-Ti basalts must account for most of the filling of Mare Fecunditatis. The fields of medium-to high-Ti basalts appear spatially related to thick basalt accumulations. The units with higher Ti content cover smaller area than units with lower Ti content and are nested in the lower Ti units. Such a spatial relationship suggests that volcanism in the mare started with voluminous low-Ti lavas. The lavas gradually evolved toward higher titanium content, and the lava production was gradually decreasing with time until it terminated with small volume of localized high-Ti lavas. The sources of the lavas could be linear features such as the one south of Taruntius crossing the units #62, #60, and #50, along which mostly low-Ti basalt crops out in the southeast. Toward the northwest this basalt becomes richer in Ti. Another such linear feature in the units #49 and #46 could be the source for the high-Ti units spreading toward the southeast (Fig.13).

This scenario should be tested against the age data as in Mare Tranquillitatis. Unfortunately, dating with a high spatial resolution has not been done yet. Boyce (1976) recognized two units in Mare Fecunditatis with different ages based on crater counts. According to his study, most of the basalts in the mare formed at 3.4 ± 0.1 Ga (not indicated whether 1 or 2 σ). A small area in the NE (which includes our easternmost green units and yellow and orange units farther east) formed at 3.6 ± 0.1 Ga. The Basaltic Volcanism Study Project (1981) placed all basalts within the mare at 3.2–3.7 Ga. Radiometric dating of Luna 16 basalts (~5 wt% TiO_2) recognized three volcanic events at 3.155 ± 0.004 Ga, 3.347 ± 0.024 Ga, and 3.421 ± 0.030 Ga (Cohen et al. 2001). Lack of published chemical data for the dated samples did not allow us to explore the chemical evolution of the Fecunditatis basalts as we did for Mare Tranquillitatis.

Kodama and Yamaguchi (2003) reached similar conclusions about the connectivity of the low-Ti basalts between M. Fecunditatis and M. Tranquillitatis and the stratigraphic relationships. However, their conclusion of Fc3 being older than Fc4 is not consistent with our interpretation.

CONCLUSION

Iron distribution patterns in Maria Tranquillitatis and Fecunditatis are strongly controlled by local impact excavation of iron-poor basement from beneath basalt flows (i.e., vertical mixing), but at some areas the iron distribution is mainly controlled by ejecta of large impact craters (i.e., lateral mixing). Titanium content of mare soils is generally lowered by locally excavated basement material, but the relative distribution of titanium is controlled by the composition of underlying basalt and ejecta of large impact craters.

Basalts in both maria contain mostly 18–19 wt% FeO, in places as low as 16 wt% FeO, and from nearly 0 to 11 wt% TiO_2. Volcanism in both maria started with low-Ti basalts and evolved toward medium- and high-Ti basalts. However, some of the high-Ti basalts in Mare Tranquillitatis began erupting quite early, contemporaneously with the low- and medium-Ti basalts, and even form the oldest units exposed on mare surface. Mare Tranquillitatis is mostly covered with high-Ti basalts. In Mare Fecunditatis, the volume of erupting basalts clearly decreased with increased titanium content, and the high-Ti basalts form only a few patches on the mare surface.

The total basalt thickness in Mare Tranquillitatis varies about a mean of several hundred meters, the eastern part of the mare being shallower than the western part. The thickness varies locally and in the northwest is up to 1200–1600 m. Mare Fecunditatis basalts are also several hundred meters thick and at several local accumulations are more than 1000-m thick. The new basalt thickness estimates generally fall within the range set by earlier studies although they differ locally.

The medium- to high-Ti basalts exposed at surfaces of both maria are quite thin—meters to tens of meters thick.

Acknowledgments–We would like to thank LPI staff for technical and financial support; Brian Fessler was particularly essential for processing of the image mosaics. This project was a part of a PhD dissertation supervised by Arch Reid who also contributed to the final editing of the manuscript. D. T. Blewett and an anonymous reviewer provided valuable detailed comments that helped to improve the manuscript. LPI Contribution #1210.

Editorial Handling— Dr. Carlé Pieters

REFERENCES

Basaltic Volcanism Study Project. 1981. *Basaltic volcanism on the terrestrial planets.* New York: Pergamon Press, Inc. 1286 p.

Blewett D. T., Lucey P. G., Hawke B. R., and Jolliff B. L. 1997. Clementine images of the lunar sample-return stations: Refinement of FeO and TiO_2 mapping techniques. *Journal of Geophysical Research* 102:16319–16325.

Boyce J. M. 1976. Ages of flow units in the lunar nearside maria based on Lunar Orbiter IV photographs. Proceedings, 7th Lunar and Planetary Science Conference. pp. 2717–2728.

Budney C. J. and Lucey P. G. 1998. Basalt thickness in Mare Humorum: The crater excavation method. *Journal of Geophysical Research* 103:16,855–16,870.

Chambers J. G., Taylor L. A., and Patchen A. 1995. Quantitative mineralogical characterization of lunar high-Ti mare basalts and soils for oxygen production. *Journal of Geophysical Research*

100:14391–14402.
Cohen B. A., Snyder G. A., Hall C. M., Taylor L. A., and Nazarov M. A. 2001. Argon-40-argon-39 chronology and petrogenesis along the eastern limb of the Moon from Luna 16, 20, and 24 samples. *Meteoritics & Planetary Science* 36:1345–1366.
DeHon R. A. 1974. Thickness of mare material in the Tranquillitatis and Nectaris basins. Proceedings, 5th Lunar and Planetary Science Conference. pp. 53–59.
DeHon R. A. and Waskom J. D. 1976. Geologic structure of the eastern mare basins. Proceedings, 7th Lunar and Planetary Science Conference. pp. 2729–2746.
Essene E. J., Ringwood A. E., and Ware N. G. 1970. Petrology of the lunar rocks from Apollo 11 landing site. Proceedings, 1st Lunar Science Conference. pp. 385–397.
Farrand W. H. 1988. Highland contamination and minimum basalt thickness in northern Mare Fecunditatis. Proceedings, 18th Lunar and Planetary Science Conference. pp. 319–329.
Gibson M. A. and Knudsen C. W. 1985. Lunar oxygen production from ilmenite (abstract). In *Lunar bases and space activities of the 21st century,* edited by Mendell W. W. Houston, Texas: Lunar and Planetary Institute. p. 26.
Gifford A. W. and El-Baz F. 1981. Thicknesses of lunar mare flow fronts. *The Moon and the Planets* 24:391–398.
Giguerre T. A., Taylor G. J., Hawke B. R., and Lucey P. G. 2000. The titanium contents of lunar mare basalts. *Meteoritics & Planetary Science* 35:193–200.
Greeley R., Kadel S. D., Williams D. A., Gaddis L. R., Head J. W., McEwen A. S., Murchie S. L., Nagel E., Neukum G., Pieters C. M., Sunshine J. M., Wagner R., and Belton M. J. S. 1993. Galileo imaging observations of Lunar Maria and related deposits. *Journal of Geophysical Research* 98:17,183–17,206.
Grieve R. A. F., Robertson P. B., and Dence M. R. 1981. Constraints on the formation of ring impact structures, based on terrestrial data. Proceedings, 12th Lunar and Planetary Science Conference. pp. 37–58.
Hawke B. R., Blewett D. T., Lucey P. G., Peterson C. A., Bell J. F., III, Campbell B. A., and Robinson M. S. 1999. The composition and origin of selected lunar crater rays (abstract). In *New views of the Moon II workshop, e*dited by Gaddis L. R. and Shearer C. K. LPI Contribution #980. pp. 22–23.
Head J. W. 1982. Lava flooding of ancient planetary crusts: Geometry, thickness, and volumes of flooded lunar impact basins. *The Moon and the Planets* 26:61–88.
Heiken G. T., Vaniman D. T., and French B. M. 1991. Lunar sourcebook: *A user's guide to the Moon.* Cambridge: Cambridge University Press. 736 p.
Hiesinger H., Jaumann R., Neukum G., and Head J. W. III. 1998. On the relation of age and titanium content of lunar mare basalts (abstract #1243). 29th Lunar and Planetary Science Conference. CD-ROM.
Hiesinger H., Jaumann R., Neukum G. and Head J. W. III. 2000. Ages of mare basalts on the lunar nearside. *Journal of Geophysical Research* 105:29239–29275.
Hiesinger H., Head J. W., III, Wolf U., Jaumann R., and Neukum G. 2001. Lunar mare basalts: Mineralogical variations with time (abstract #1826). 32nd Lunar and Planetary Science Conference. CD-ROM.
Hiesinger H., Head J. W. III, Wolf U., Jaumann R., and Neukum G. 2002. Lunar mare basalt flow units: Thicknesses determined from crater size-frequency distributions. *Geophysical Research Letters* 29:89-1–89-4.
Hörz F. 1978. How thick are lunar mare basalts? Proceedings, 9th Lunar and Planetary Science Conference. pp. 3311–3331.
Howard K. A., Head J. W., and Swann G. A. 1972. Geology of Hadley Rille. Proceedings, 3rd Lunar and Planetary Science Conference. pp. 1–14.
Jakeš P., Warner J., Ridley W. I., Reid A. M., Harmon R. S., and Brett R. 1972. Petrology of a portion of the Mare Fecunditatis regolith. *Earth and Planetary Science Letters* 13:257–271.
Jerde E. A., Snyder G. A., Taylor L. A., Liu Y.-G., and Schmitt R. A. 1994. The origin and evolution of lunar high-Ti basalts: Periodic melting of a single source at Mare Tranquillitatis. *Geochimica et Cosmochimica Acta* 58:515–527.
Johnson J. R., Larson S. M., and Singer R. B. 1991. Remote sensing of potential lunar resources 1. Near-side compositional properties. *Journal of Geophysical Research* 96:18861–18882.
Kodama S. and Yamaguchi Y. 2003. Lunar mare volcanism in the easternside region derived from Clementine UV/VIS data. *Meteoritics & Planetary Science* 38:1461–1484.
Konopliv A. S., Asmar S. W., Carranza E., Sjogren W. L., and Yuan D. N. 2001. Recent gravity models as a result of the Lunar Prospector mission. *Icarus* 150:1–18.
Lemoine F. G. R., Smith D. E., Zuber M. T., Neumann G. A., and Rowlands D. D. 1997. A 70th degree lunar gravity model (GLGM-2) from Clementine and other tracking data. *Journal of Geophysical Research* 102:16339–16359.
Li L. and Mustard J. F. 2000. The compositional gradients and lateral transport by dark-halo and dark-ray craters (abstract #2007). 31st Lunar and Planetary Science Conference. CD-ROM.
Lucey P. G., Taylor G. J., and Malaret E. 1995. Abundance and distribution of iron on the Moon. *Science* 268:1150–1153.
Lucey P. G., Blewett D. T., and Hawke B. R. 1998. Mapping the FeO and TiO_2 content of the lunar surface with multispectral imagery. *Journal of Geophysical Research* 103:3679–3699.
Lucey P. G., Blewett D. T., and Jolliff B. L. 2000a. Lunar iron and titanium abundance algorithms based on final processing of Clementine ultraviolet images. *Journal of Geophysical Research* 105:20297–20305.
Lucey P. G., Blewett D. T., Taylor G. J., and Hawke B. R. 2000b. Imaging of lunar surface maturity. *Journal of Geophysical Research* 105:20377–20386.
Maxwell D. E. 1977. Simple Z model of cratering, ejection, and the overturned flap. In *Impact and explosion cratering,* edited by Roddy D. J., Pepin R. O., and Merrill R. B. New York: Pergamon Press. pp. 1003–1008.
Melendrez D. E., Johnson J. R., Larson S. M., and Singer R. B. 1994. Remote sensing of potential lunar resources 2. High spatial resolution mapping of spectral reflectance ratios and implications for nearside mare TiO_2 content. *Journal of Geophysical Research* 99:5601–5619.
Melosh H. J. 1989. *Impact cratering: A geologic process,* 1st ed. New York: Oxford University Press. 245 p.
Mustard J. F. and Head J. W. 1996. Buried stratigraphic relationships along the southwestern shores of Oceanus Procellarum: Implications for early lunar volcanism. *Journal of Geophysical Research* 101:18913–18925.
Mustard J. F., Li L., and He G. 1998. Nonlinear spectral mixture modeling of lunar multispectral data: Implications for lateral transport. *Journal of Geophysical Research* 103:19419–19425.
Nyquist L. E. and Shih C.-Y. 1992. The isotopic record of lunar volcanism. *Geochimica et Cosmochimica Acta* 56:2213–2234.
Pieters C. M. 1978. Mare basalt types on the front side of the Moon: A summary of spectral reflectance data. Proceedings, 9th Lunar and Planetary Science Conference. pp. 2825–2849.
Pieters C. M., Adams J. B., Smith M. O., Mouginis-Mark P. J., and Zisk S. H. 1985. The nature of crater rays—The Copernicus example. *Journal of Geophysical Research* 90:12393–12413.
Rhodes J. M. 1977. Some compositional aspects of lunar regolith

evolution. *Philosophical Transactions of the Royal Society of London A* 285:293–301.

Schaber G. G., Boyce J. M., and Moore H. J. 1976. The scarcity of mappable flow lobes on the lunar maria: Unique morphology of the Imbrium flows. Proceedings, 7th Lunar and Planetary Science Conference. pp. 2783–2800.

Sjogren W. L., Wimberly R. N., and Wollenhaupt W. R. 1973. Lunar gravity via the Apollo 15 and 16 subsatellites. *The Moon* 9:115–128.

Staid M. I., Pieters C. M., and Head J. W. III. 1996. Mare Tranquillitatis: Basalt emplacement history and relation to lunar samples. *Journal of Geophysical Research* 101:23213–23228.

Taylor G. J., Warren P., Ryder G., Delano J., Pieters C. M., and Lofgren G. 1991. Lunar rocks. In *Lunar sourcebook: A user's guide to the Moon,* edited by Heiken G. T., Vaniman D. T., and French B. M. Cambridge: Cambridge University Press. pp. 183–284.

Thurber C. H. and Solomon S. C. 1978. An assessment of crustal thickness variations on the lunar near side—Models, uncertainties, and implications for crustal differentiation. Proceedings, 9th Lunar and Planetary Science Conference. pp. 3481–3497.

Wilhelms D. 1987. The geologic history of the Moon. USGS Profesional Paper 1348. Denver: U.S. Geological Survey. 302 p.

Williams D. A., Greeley R., Neukum G., Wagner R., and Kadel S. D. 1995. Multispectral studies of western limb and farside maria from Galileo Earth-Moon Encounter 1. *Journal of Geophysical Research* 100:23,291–23,300.